

Supporting Information

**Desolvation-Based Molecular Crowding Mechanism Revealed through TmPyP–Zn**

**Complexation in Alcohols**

Akihisa Miyagawa<sup>1\*</sup>, Chisa Ito<sup>2</sup>, Shigenori Nagatomo<sup>2</sup>, Kiyoharu Nakatani<sup>2</sup>.

1: Department of Chemistry, Graduate School of Advanced Science and Engineering,

Hiroshima University, 1-3-1 Kagamiyama, Higashi-Hiroshima, 739-8526, Japan.

Tel.: +81-82-424-7426

Email: miyagawaaki@hiroshima-u.ac.jp

2: Department of Chemistry, Faculty of Pure and Applied Sciences, University of

Tsukuba, Tsukuba, Ibaraki 305-8571, Japan

Table S1. Summary of the  $\epsilon$  values of Soret band of TMPyP complex in the organic solvent at various  $C_{\text{PEG}}$ .

$C_{\text{PEG}} / \text{vol}\%$	$\epsilon / \text{M}^{-1} \text{cm}^{-1}$		
	MeOH	EtOH	PrOH
0	138000	81200	184000
2.5	-	91900	197000
5.0	-	88500	167000
7.5	-	87800	173000
10	129000	76700	169000
15	-	81000	185000
20	139000	82000	-
30	112000	79800	-
40	113000	-	-
50	125000	-	-

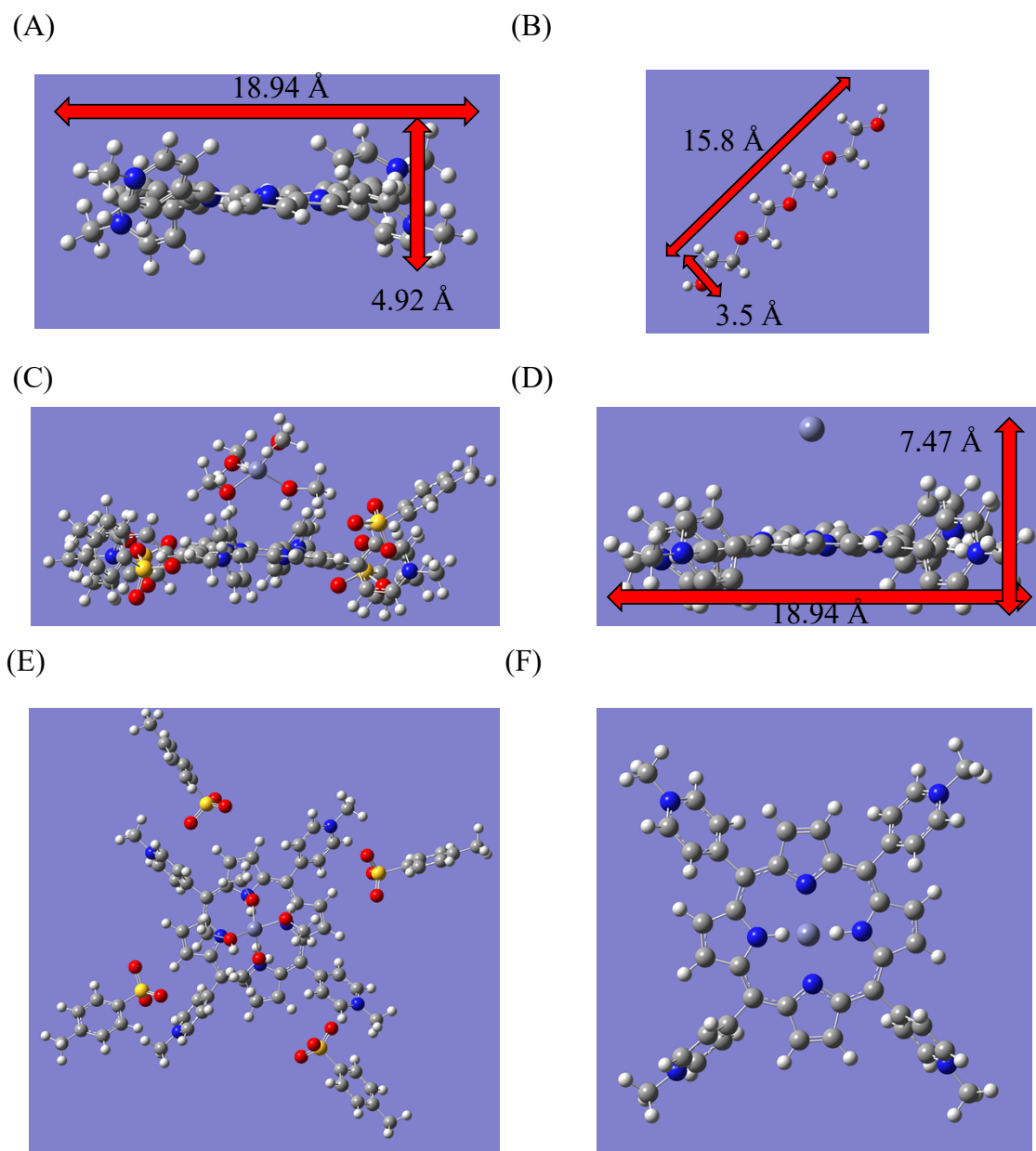


Figure S1 Optimized structures of (A) TMPyP, (B) PEG200, (C) the full TMPyP-Zn ionic pair (side view), (D) the simplified TMPyP-Zn ionic pair in which TsO<sup>-</sup> and methanol molecules are omitted (side view), (E) the full TMPyP-Zn ionic pair (top view), and (F) the simplified TMPyP-Zn ionic pair in which TsO<sup>-</sup> and methanol molecules are omitted (top view), obtained from DFT calculations performed using Gaussian 16.

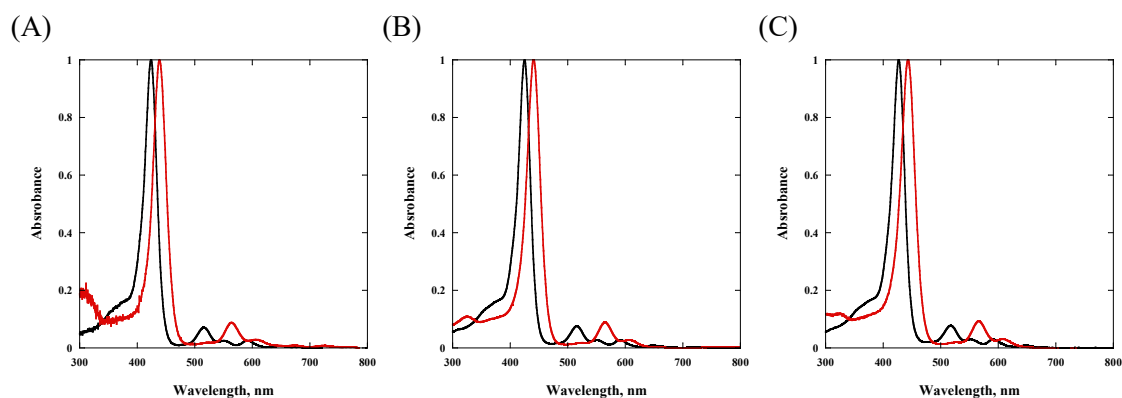


Figure S2. Normalized absorption spectra of raw TMPyP (black) and TMPyP complex with  $\text{Zn}^{2+}$  (red) in (A) MeOH, (B) EtOH, and (C) PrOH solutions at 25 °C. The Soret band ( $\sim 420$  nm) and Q bands (500–650 nm) of free TMPyP, attributed to  $\pi$ – $\pi$  transitions, exhibit red shifts upon complexation with  $\text{Zn}^{2+}$ . The Soret maxima of the TMPyP–Zn complex appear at 438 nm (MeOH), 440 nm (EtOH), and 443 nm (PrOH). Wavelengths of 450 nm (MeOH), 455 nm (EtOH), and 450 nm (PrOH) were selected for kinetic analysis to minimize interference from unreacted TMPyP.

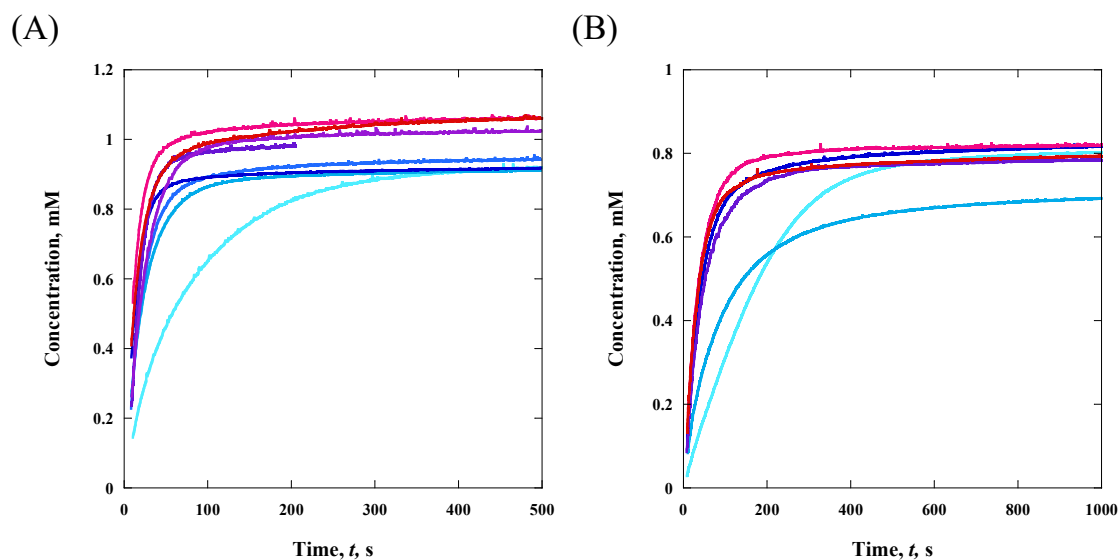


Figure S3. (A) Time-dependent concentration profiles of the TMPyP–Zn complex in EtOH and (B) PrOH at 25 °C under various  $C_{\text{PEG}}$ . Reaction conditions were identical to those in Figure 1 (final  $\text{Zn}^{2+}$  concentration 1  $\mu\text{M}$ ; TMPyP 5.92  $\mu\text{M}$ ). Curves are shown for  $C_{\text{PEG}} = 0, 2.5, 5.0, 7.5, 10, 15, 20,$  and 30 vol% in EtOH, and 0, 2.5, 5.0, 7.5, 10, and 15 vol% in PrOH (sky-blue to red). Increasing  $C_{\text{PEG}}$  reduces the time required to reach equilibrium, demonstrating that molecular crowding accelerates the complexation kinetics in both solvents, although the baseline rates differ depending on solvent identity.

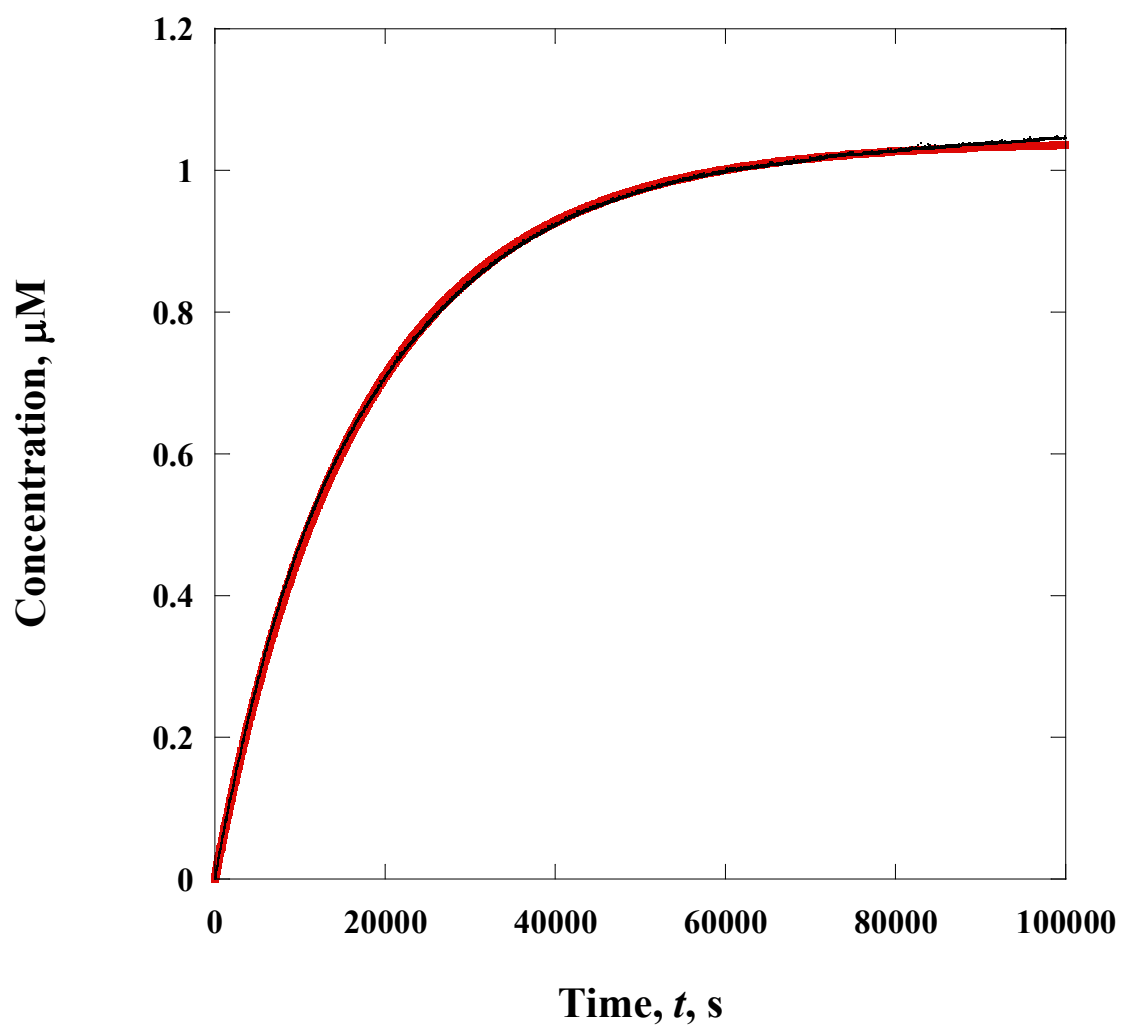


Figure S4. Time-dependent concentrations of TMPyP complex in MeOH solution at  $C_{\text{PEG}} = 0\text{vol}\%$ . The black plots were experimental results. The red curve presents the curve-fitted result based on Eqs. (3)-(6) using  $k_1 = 4.72 \times 10^{-3} \text{ M}^{-1} \text{ s}^{-1}$ ,  $k_{-1} = 0.456 \text{ s}^{-1}$ , and  $k_2 = 1.0 \times 10^{-4} \text{ s}^{-1}$  as fitting parameters.

Table S2. Summary of the  $k$  values.

Solvent	$C_{\text{PEG}} / \text{vol}\%$	$k_1 / \text{M}^{-1} \text{s}^{-1}$	$k_{-1} / \text{s}^{-1}$	$k_2 / \text{s}^{-1}$
MeOH	0	$(3.05 \pm 1.44) \times 10^{-3}$	$0.858 \pm 0.403$	$(3.13 \pm 1.84) \times 10^{-3}$
	10	$(7.72 \pm 1.94) \times 10^{-2}$	$3.04 \pm 1.82$	$(6.48 \pm 2.93) \times 10^{-3}$
	20	$(1.69 \pm 0.66) \times 10^{-1}$	$4.31 \pm 0.30$	$(5.32 \pm 2.21) \times 10^{-3}$
	30	$(8.77 \pm 2.75) \times 10^{-2}$	$5.16 \pm 0.09$	$(1.03 \pm 0.35) \times 10^{-2}$
	40	$(4.50 \pm 0.89) \times 10^{-2}$	$7.58 \pm 2.62$	$0.119 \pm 0.081$
	50	$(4.06 \pm 0.40) \times 10^{-2}$	$11.2 \pm 1.3$	$0.426 \pm 0.024$
EtOH	0	$0.204 \pm 0.082$	$4.61 \pm 0.27$	$0.0474 \pm 0.0087$
	2.5	$0.252 \pm 0.081$	$4.25 \pm 0.36$	$0.105 \pm 0.005$
	5	$0.210 \pm 0.007$	$4.40 \pm 0.04$	$0.126 \pm 0.013$
	7.5	$0.272 \pm 0.020$	$4.06 \pm 0.09$	$0.155 \pm 0.026$
	10	$0.192 \pm 0.027$	$4.49 \pm 0.12$	$0.127 \pm 0.015$
	15	$0.317 \pm 0.257$	$4.04 \pm 0.97$	$0.116 \pm 0.038$
	20	$0.289 \pm 0.028$	$6.65 \pm 4.89$	$0.339 \pm 0.030$
	30	$0.366 \pm 0.113$	$12.1 \pm 0.4$	$0.201 \pm 0.044$
PrOH	0	$0.116 \pm 0.014$	$3.99 \pm 0.01$	$(4.02 \pm 0.57) \times 10^{-2}$
	2.5	$0.209 \pm 0.044$	$4.43 \pm 0.22$	$(7.90 \pm 0.52) \times 10^{-2}$
	5	$0.184 \pm 0.048$	$4.59 \pm 0.22$	$(7.27 \pm 1.73) \times 10^{-2}$
	7.5	$0.179 \pm 0.035$	$4.62 \pm 0.17$	$(6.93 \pm 1.17) \times 10^{-2}$
	10	$0.201 \pm 0.046$	$4.49 \pm 0.17$	$(8.23 \pm 2.41) \times 10^{-2}$
	15	$0.181 \pm 0.020$	$4.64 \pm 0.02$	$(8.53 \pm 1.57) \times 10^{-2}$

Parenthesis represent the standard deviations in three independent measurements.

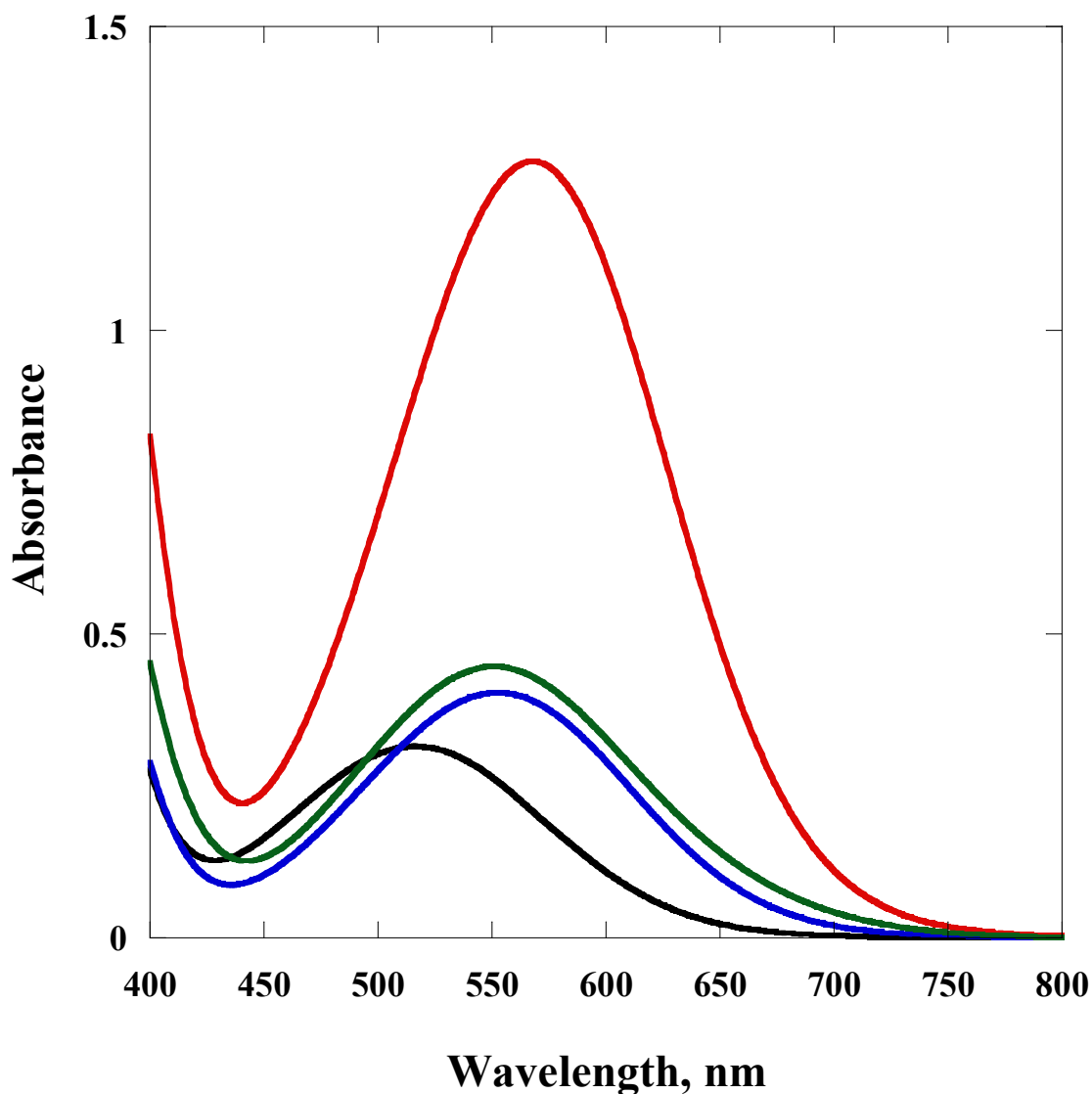


Figure S5. Absorption Spectra of Reichardt's dye in MeOH (black), EtOH (blue), PrOH (red), and PEG200 (green). The charge-transfer band maxima were observed at 515.5 nm (MeOH), 553.5 nm (EtOH), 568 nm (PrOH), and 550.5 nm (PEG200). The corresponding empirical polarity parameters ( $E_t$  values) were calculated from the absorption maxima and used to evaluate changes in solvent polarity upon PEG200 addition. The results indicate that although the overall polarity differences among the solvents and PEG200 are modest, MeOH exhibits a larger deviation, suggesting higher sensitivity to polarity changes.

Table S3. Summary of the  $\gamma_{\text{sol}}$  values.

Solvent	$C_{\text{PEG}} / \text{vol}\%$	$\gamma_{\text{sol}}$
MeOH	0	1.00
	10	0.977
	20	0.955
	30	0.934
	40	0.913
	50	0.892
EtOH	0	1.00
	2.5	0.992
	5	0.984
	7.5	0.976
	10	0.967
	15	0.952
	20	0.936
	30	0.906
PrOH	0	1.00
	2.5	0.990
	5	0.979
	7.5	0.969
	10	0.959
	15	0.939

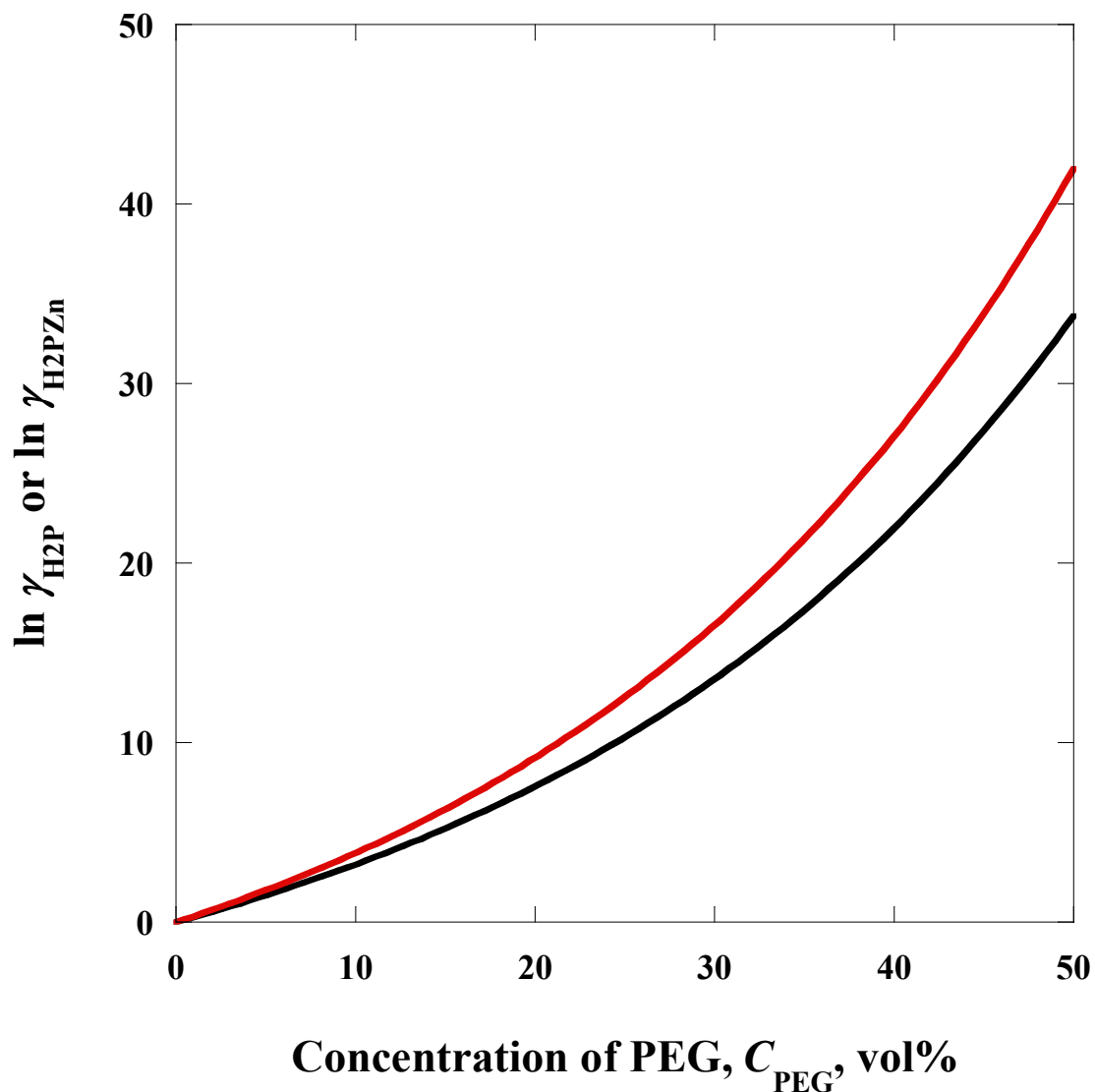


Figure S6. Relationship between  $C_{\text{PEG}}$  and  $\ln \gamma_{\text{H}_2\text{P}}$  (black) or  $\ln \gamma_{\text{H}_2\text{P}\cdot\text{Zn}}$  (red) calculated based on the hard-particle excluded-volume model are shown as a function of  $C_{\text{PEG}}$ . The increase in  $\gamma$  values with increasing  $C_{\text{PEG}}$  reflects the enhanced effective concentration of solute species due to volume exclusion by PEG200. The growing difference between  $\gamma_{\text{H}_2\text{P}}$  and  $\gamma_{\text{H}_2\text{P}\cdot\text{Zn}}$  at higher  $C_{\text{PEG}}$  indicates a decrease in  $I_1$ , consistent with suppression of ion-pair formation by excluded-volume effects.